Degradation and failure mechanisms of P-GaN HEMTs in single and complex radiation environments *

Yong-chang Sun,[1] Ying Wang,[1, †] Wan-zhao Cui,[2] Huo-lin Huang,[3] Yan-xing Song,[1] and Fei Cao[1]

[1]*School of Information Science and Technology, Dalian Maritime University, Dalian 116026, China*

[2]*National Key Laboratory of Science and Technology on Space Microwave, China Academy of Space Technology (Xi'an), Xi'an 710100, China*

[3]*School of Optoelectronic Engineering and Instrumentation Science, Dalian University of Technology, Dalian 116024, China*

In this work, the mechanisms of total ionizing dose effect (TID) and single-event burnout (SEB) failure in P-type gallium nitride gate high electron mobility transistors (P-GaN HEMTs) was investigated based on experiment and simulation. In the TID experiments, three groups of samples with different voltage bias were irradiated up to a maximum of $1\ \mathrm{Mrad(Si)}$ using ^{60}Co γ-rays with an average energy of $1.25\,\mathrm{MeV}$, at a dose rate of 100 rad(Si)/s. Positive threshold voltage shifts of different magnitudes are observed, while the gate leakage current increases insignificantly in all of them. We believe that electron and hole trapping at the P-GaN/AlGaN interface and in the AlGaN barrier layer is the main reason for the threshold voltage shift. For the SEB experiments, a tantalum (Ta) ion beam was used for irradiation at an energy of $854.3\,\mathrm{MeV}$ and Linear Energy Transfer (LET) value of $86.8\,\mathrm{MeVcm^2/mg}$ in silicon. When the drain-source voltage was $350\,\mathrm{V}$, we observed a significant surge in drain current, while the gate current did not show an uncontrollable increase. The simulation results indicate that the local electric field enhancement due to charge enhancement effect and charge collection phenomenon as well as the intensification of collisional ionization are the main causes of device damage and failure. In addition, we subjected one of the three groups of samples that had undergone TID experiments to Ta ion single-event effect (SEE) experiments once again. The synergistic experimental results show the superposition effect of the two experiments.

Keywords: High electron mobility transistors, single-event burnout, total ionizing dose effect, synergistic effect.

I. INTRODUCTION

With the rapid development of aerospace and deep space exploration technologies, the performance demand of spacecraft energy power systems is increasing. Compared with the traditional silicon-based power devices, gallium nitride (GaN) power devices have become a research hotspot in this field by virtue of their significant advantages such as high operating voltage, high power density and high operating frequency [1–5]. GaN material has the characteristics of high critical electric field strength and high atomic displacement threshold, which make it show unique advantages in aerospace high-power applications [6–9]. However, limited by the maturity of the current fabrication process, the performance potential of GaN power devices has not been fully released. In addition, in the space radiation environment, the irradiation effect of high-energy particles and rays will lead to device performance degradation or even failure, mainly manifested in the single-event effect (SEE), the total ionizing dose effect (TID) and displacement damage (DD) [10–13]. These factors seriously restrict the wide application of GaN power devices in the aerospace field.

The sensitivity of gallium nitride high electron mobility transistors (GaN HEMTs) to TID effect is affected by a variety of factors, especially under high-voltage and high-field operating conditions, where the coupling of the radiation effect with the internal electric field of the device makes the radiation damage mechanism more complicated. Y. P. Wang et al. [14] conducted γ-ray irradiation experiments on GaN HEMTs under different bias conditions (off-state, open-state, and float), and found that the electrical parameters of the devices under the float condition were the most stable after irradiation, and almost no obvious radiation damage was observed; the device performance degradation under the off-state condition was the second most important, and that of the devices under the open-state condition was the most significant. R. Jiang et al. [15] conducted X-ray and γ-ray irradiation experiments on the depletion-mode GaN HEMTs from the laboratory, Cree, and Qorvo. The results showed that the threshold voltages of different devices showed different degrees of negative drift phenomena. Wu et al. [16]carried out TID experiments for P-GaN HEMT devices with different gate voltage biases, and found that the amount of negative drift in the threshold voltage is independent of the breakdown voltage of the device, but mainly depends on the magnitude of the applied gate voltage.

Several research teams have carried out studies on the single-event effect in GaN power devices. Cai et al. [17]first investigated the degradation behavior of single-particle effect in AlGaN/GaN HEMTs by proton irradiation experiments and reported a significant decrease in the transconductance and DC output current. Y. Wang et al. [18]systematically investigated the single-particle-incidence sensitive region of GaN MISFET devices and its burnout mechanism, and significantly improved the burnout threshold voltage of the devices by introducing a Schottky electrode to rapidly discharge irradiation-induced non-equilibrium carriers. Z. X. Zhen et al. [19]further pointed out that the gate edge region is the single-particle-incidence sensitive location of P-GaN HEMT

* This work was supported in part by National R&D Program for Major Research Instruments of China (Grant No. 62027814).

† Corresponding author, wangying7711@dlmu.edu.cn

devices, and effectively suppressed the collisional ionization effect in the high electric field region using a multi-field plate structure. However, the existing studies mainly focus on the exploration and validation of the device burnout mechanism and reinforcement technology based on simulation software, and the experimental studies on the SEB induced by heavy ions (e.g., Ta ions) are still relatively scarce, which are urgently needed for further in-depth exploration.

In this work, we performed γ-ray and Ta ions irradiation experiments on the same samples and observed TID degradation and SEB failure phenomena respectively. In addition, the samples after the TID experiments were subjected to SEE experiments, which revealed the degradation effect due to the synergistic effect and provided a rational explanation.

II. TID EXPERIMENT TEST AND ANALYSIS

1. *Device information and experimental setups*

The P-GaN HEMT samples used in the experiments were designed with a multilayer heterostructure as shown in Fig. 1. A $50\,\mathrm{nm}$ AlN nucleation layer, a $5.8\,\mu\mathrm{m}$ GaN buffer layer, a $200\,\mathrm{nm}$ non-doped GaN channel layer, a $15\,\mathrm{nm}$ $Al_{0.25}Ga_{0.75}N$ barrier layer, and $110\,\mathrm{nm}$ Mg-doped P-GaN layer were sequentially epitaxially grown on a sapphire substrate . The devices have a source-drain spacing of $2\,\mu\mathrm{m}$, a gate-drain spacing of $7\,\mu\mathrm{m}$, and a field plate length of $4\,\mu\mathrm{m}$.

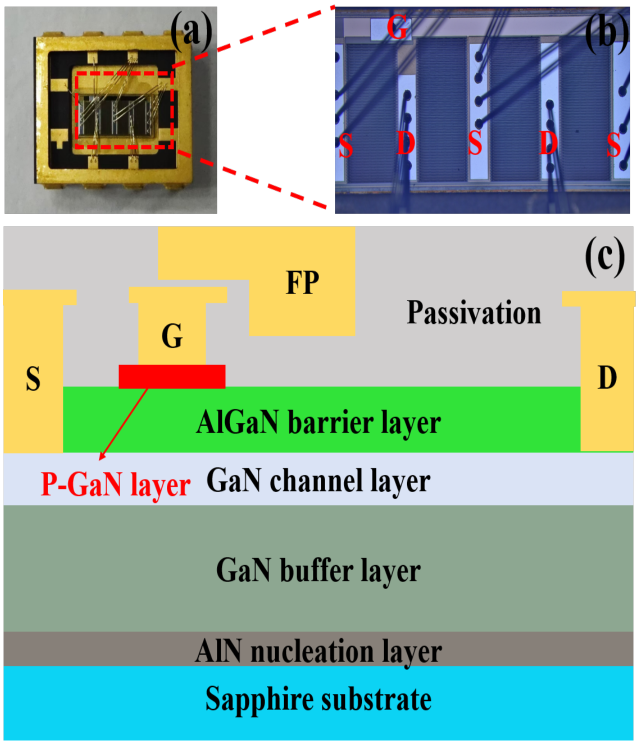

Fig. 1. Appearance (a), package diagram (b) and schematic structure (c) of P-GaN HEMT samples.

The TID experiment was conducted under a ^{60}Co γ-ray source selected with a dose rate set at $100\ \mathrm{rad(Si)/s}$ and the experimental environment is shown in the Fig. 2 (a). According to the applied voltage bias, the experimental samples were divided into three groups: GND, Semi-ON and ON. The bias conditions of the devices are shown in Table 1 below. The samples were irradiated up to a maximum dose of $1\ \mathrm{Mrad(Si)}$ and we choose $100\ \mathrm{Krad(Si)}$, $300\ \mathrm{Krad(Si)}$, $500\ \mathrm{Krad(Si)}$ and $700\ \mathrm{Krad(Si)}$ as the intermediate doses. These samples were systematically characterized electrically using a Keithley SCS-4200 Semiconductor Parameter Analyzer, as shown in Fig. 2 (b), before and after the irradiation experiment, and all the tests were carried out at room temperature.

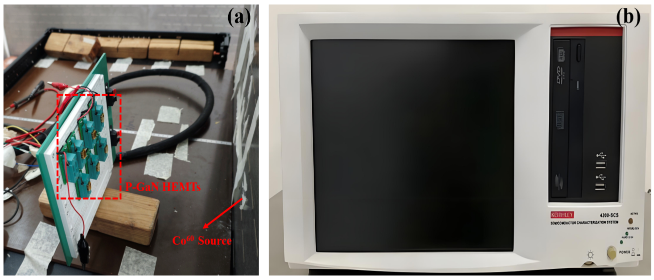

Fig. 2. TID experimental environment (a) and Keithley SCS-4200 Semiconductor Parameter Analyzer (b).

TABLE 1. Different voltage biases of devices in TID experiment.

	Vgs(V)	Vds(v)
GND	0	0.1
Semi-ON	1.5	0.1
ON	2	0.1

2. *Results and analysis of TID experiment*

Threshold voltage instability is one of the inherent reliability issues of semiconductor devices [20, 21]. The Fig. 3. demonstrates the threshold voltage drift under three different gate bias conditions. The positive threshold voltage drift phenomenon is observed in all of them, and the threshold voltage drift tends to increase monotonically with the increase of γ-ray irradiation dose. In addition, we also found that the positive gate bias voltage applied during irradiation has a significant effect on the threshold voltage drift, which is manifested by the increase of the threshold voltage drift with the increase of the gate bias voltage. It is noteworthy that no saturation of the threshold voltage offset was observed in the dose range studied in this experiment.

Fig. 4 shows the energy band schematic of the p-GaN HEMTs under positive gate bias condition. Under the effect of high electric field applied to the gate, the channel electrons migrate toward the gate, and some of them are trapped by the acceptor traps at the P-GaN/AlGaN interface. These

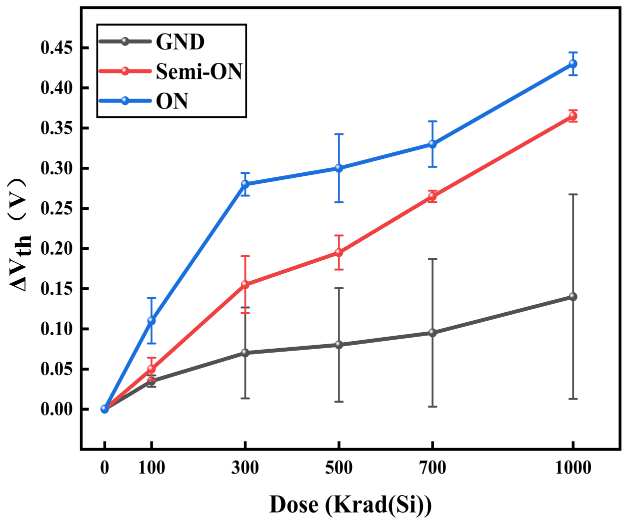

Fig. 3. Threshold voltage drift under three different bias conditions: GND, Semi-ON and ON.

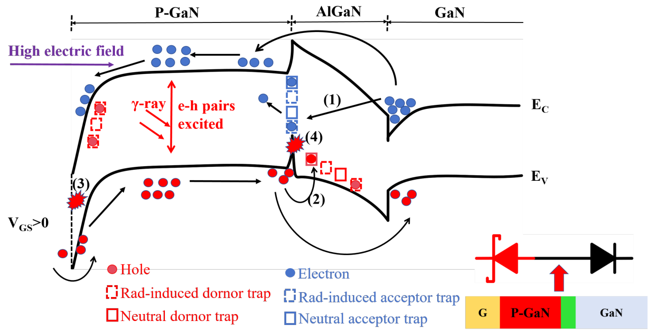

Fig. 4. Degradation mechanism under positive gate bias and gate stack equivalence diagram.

interfacial traps mainly originate from two aspects: one is the intrinsic interfacial states introduced by the imperfect surface treatment process during device fabrication; the other is the additional interfacial states induced by γ-ray irradiation at P-GaN/AlGaN interface [22]. At the same time, the irradiation-excited holes and gate-injected holes in the valence band accelerate toward the AlGaN barrier layer and release energy into the lattice through phonon emission, a process that may lead to the creation of new defects at the P-GaN/AlGaN interface (Process (4)). These interfacial states can serve as effective electron trapping centers (Process (1)). In addition, holes injected from the gate are trapped by the intrinsic as well as irradiation-induced generation of donor traps in the AlGaN layer (Process (2)) [23]. It is worth noting that the electron trapping effect in Process (1) leads to a positive threshold voltage drift, while the hole trapping effect in Process (2) causes a negative threshold voltage drift, and these two competing mechanisms together determine the threshold voltage drift characteristics of p-GaN HEMTs [24]. The experimentally observed net threshold voltage positive drift phenomenon indicates that the electron capture process dominates the competition. As the gate voltage increases, the high electric field enhances the drift motion of the electrons and the hole injection effect, resulting in the enhancement of both Processes (1) and (2), which leads to a larger amount of positive threshold voltage drift.

In order to evaluate the radiation damage characteristics of the gate stack structure, gate leakage current tests were carried out. The test results in Fig. 5 show that the gate leakage current of devices in the GND state did not show significant changes after irradiation with a total dose of $1\ \mathrm{Mrad(Si)}$. In contrast, devices in the Semi-ON and ON states exhibit specific gate leakage characteristics after irradiation: gate leakage current increases by about an order of magnitude in the gate voltage range of $1\ \mathrm{V}$ to $3\ \mathrm{V}$, while it remains essentially unchanged outside this voltage range. This phenomenon suggests that the device operating state has a significant effect on the extent of radiation damage to the gate stack, with devices under high electric field conditions being more susceptible to radiation-induced damage.

The gate stack structure of p-GaN HEMT devices can be equated to a combination of Schottky barrier diode and p-i-n diode an shown in Fig. 4. When negative bias is applied to the gate, the Schottky barrier diode is forward biased while the p-i-n diode is reverse biased, and the gate leakage current is mainly governed by the p-i-n diode. On the contrary, when a forward bias is applied to the gate, the Schottky barrier diode is reverse biased and the pin diode is forward biased, and the gate leakage current is determined by the Schottky barrier diode [25]. Experimental observations show that the reverse gate leakage current of the device does not change significantly, while the forward gate leakage current shows a slight increase. This phenomenon can be attributed to electron-hole pairs generated within the p-GaN layer during irradiation. Due to a strong electric field in space charge region of the Schottky junction, the electrons are accelerated to the metal/p-GaN interface and initiate interface damage (Process (3)). It is shown that irradiation mainly leads to degradation of the Schottky junction, while the p-i-n heterojunction function remains relatively intact. Irradiation-excited energetic electrons induce the creation of defects near the metal/p-GaN interface, which may be associated with hole trap states associated with nitrogen vacancies. Such defects can introduce a trap-assisted tunneling (TAT) mechanism that enhances the hole injection effect, leading to an increase in the forward gate current [26].

III. SEB EXPERIMENT TEST AND ANALYSIS

1. SEB experiment and simulation setups

The SEB experiment was carried out in Space Environment Simulation Research Infrastructure at Harbin Institute of Technology. The experimental environment is shown in Fig. 6(a). And a Ta ion beam with an energy of $854.3\,\mathrm{MeV}$ and Linear Energy Transfer (LET) value of $86.8\,\mathrm{MeV cm^2/mg}$ in silicon was used. The LET value of

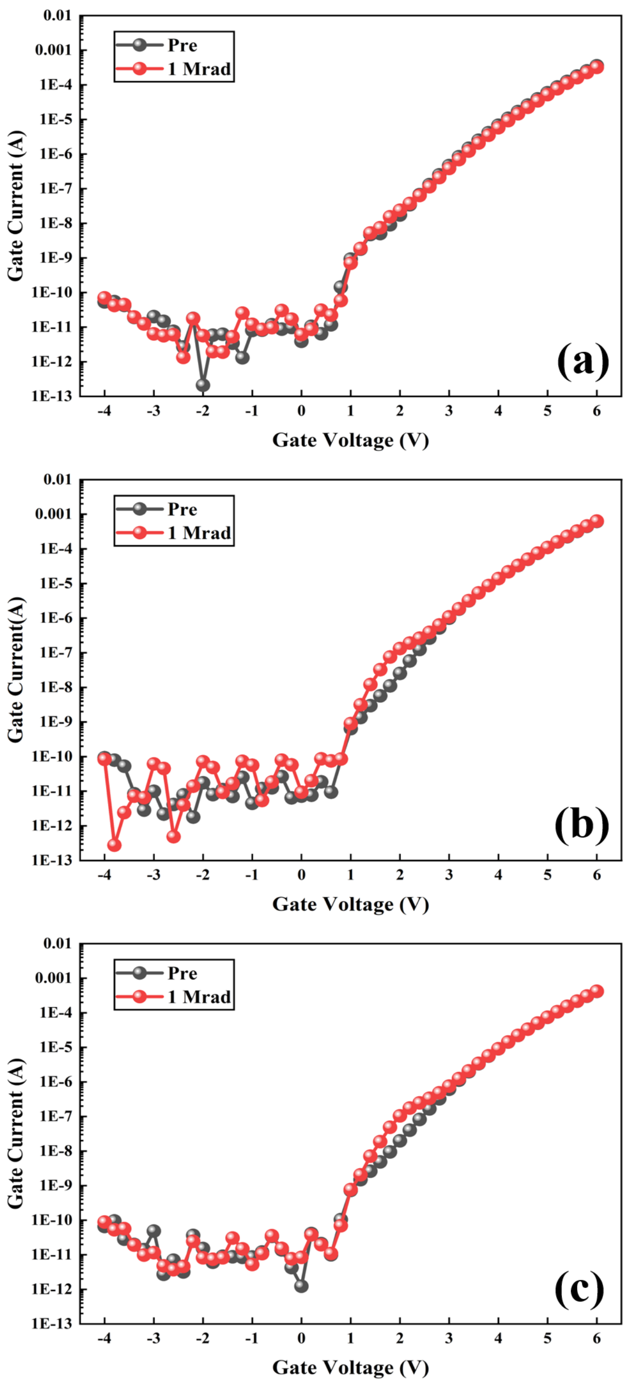

Fig. 5. Gate leakage current under three different bias conditions in TID experiments: GND (a), Semi-ON (b) and ON (c).

the Ta ion in GaN material was $66.89\,\mathrm{MeVcm^2/mg}$ calculated by SRIM. During the experiment, the ion flux was controlled at $1{\times}10^4$ ions/cm^2/s, and the duration of each irradiation stage was $100\,\mathrm{s}$ to ensure a total fluence of $1{\times}10^6$ ions/cm^2. During the irradiation process, the drain and gate bias voltages were set to $0\,\mathrm{V}$. To determine the SEB threshold voltage, the experiment was performed using the step-up method. The drain voltage was gradually increased at each irradiation stage, while the changes in drain and gate currents were monitored in real time until burnout was observed. The test system is shown in Fig. 6(b). When the current exceeds $0.1\,\mathrm{A}$, the overload protection mechanism will be triggered. And the test system will automatically disconnect the voltage bias applied to the drain. The safe drain voltage of the device under irradiation conditions was finally recorded as the basis for the evaluation of the SEB threshold voltage.

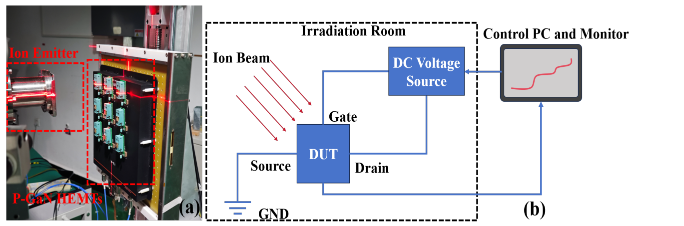

Fig. 6. SEB experimental environment diagram (a) and test system schematic diagram (b).

The 2-D TCAD simulator has been widely used to study the physical processes of SEBs and the hardening methods in power devices [27]. Therefore, we used Sentaurus TCAD to build a model of the same size as the experimental device and added the Shockley-Read-Hall (SRH) recombination, Fermi statistics, impact ionization, doping dependence, and high-field saturation mobility. The feasibility of the model has been validated in [28, 29]. Besides, a heavy-ion model was added to the simulation. For carriers induced by irradiation, the generation rate of electron–hole pairs along the track of ion incidence is described by the following equation, which uses temporal and spatial Gaussian functions [18, 30]:

$$\mathrm{rate}(x,t)=\left(\frac{\mathrm{LET}}{q\pi\,\omega_0\,T_C}\right)\exp\left[-\frac{(x-x_0)^2}{\omega_0^2}\right]\exp\left[-\frac{(t-T_0)^2}{T_c^2}\right]$$

LET and x_0 represent the LET and the incident position of heavy-ion irradiation, respectively. The initial time of the generated charge T_0 is equal to 1×10^{-13} s in this work. The spatial and temporal Gaussian function widths ω_0 and TC are set to $0.05\,\mu\mathrm{m}$ and 2×10^{-12} s, respectively. We chose the most sensitive position , the end of the field plate, as the heavy ion incidence location [31, 32]. The value of LET used in the simulations is equal to 0.635 pC/μm, which is approximately equivalent to $66.89\,\mathrm{MeVcm^2/mg}$, with a conversion factor of 0.0095 [18, 33].

2. *Results and analysis of SEB experiment*

During Ta ion beam irradiation, the samples were subjected to drain voltages ranging from $310\,\mathrm{V}$ to $350\,\mathrm{V}$, respectively. As shown in Fig. 7(a), when the drain voltage was in the range of $310\,\mathrm{V}$ to $340\,\mathrm{V}$, the transient drain current of the device showed small fluctuations and increased significantly with the increase of drain voltage, but the current overload protection was not triggered. However, when the drain voltage is increased from $340\,\mathrm{V}$ to $350\,\mathrm{V}$, the drain current increases dramatically. When irradiation was carried out up to the 24th

second at a drain voltage of 350 V, the drain current showed an uncontrollable and drastic increase, which eventually triggered the current overload protection. This phenomenon signaled the occurrence of SEB.

To determine whether the SEB event occurred in the gate region, the transient gate current was also monitored in real time during the experiment. As shown in Fig. 7(b), the transient gate current of the device exhibits small fluctuations and increases significantly with increasing drain voltage. Notably, the amplitude of the gate current is significantly higher than the drain current under the same drain voltage condition, but the current overload protection mechanism is not triggered. At a drain voltage of 350 V, the drain current did not increase dramatically when the irradiation was carried out up to the 24th second. Based on the above observations, it can be inferred that the SEB event mainly occurred in the drain region rather than the gate region.

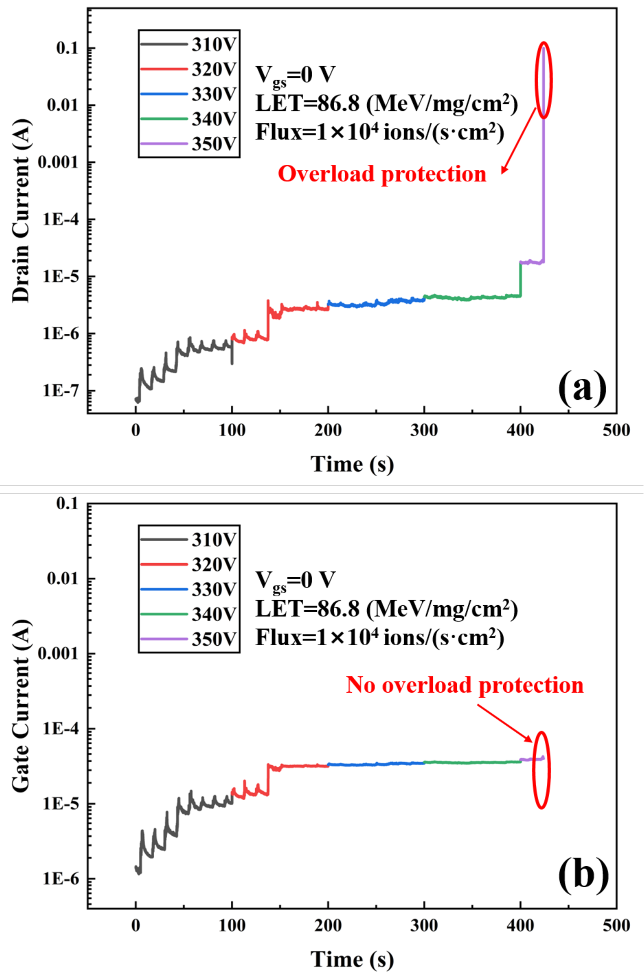

Fig. 7. Drain transient current(a) and gate transient current(b) during SEB experiments.

Subsequently, we observed the surface of the device where SEB occurred using a microscope, and the results are shown in Fig. 8. The observation shows that significant burnout damage regions appear on the device surface, and these damages are mainly concentrated in the drain region. This phenomenon further confirms that the drain region is highly sensitive to the SEB effect and is the main region of device failure. Therefore, the drain region should be used as a key region in the design of radiation reinforcement of the device in order to enhance the SEB resistance of P-GaN HEMTs.

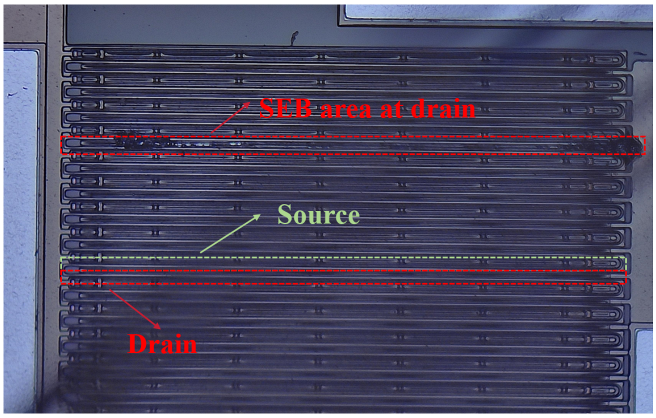

Fig. 8. Localized enlargement of the surface of the burned device.

The current simulation results of p-GaN HEMT devices are shown in Fig. 9. During the simulation, we observed that the source and the drain have two significant current density peaks when $t = 1 \times 10^{-13}$ s and $t = 2 \times 10^{-11}$ s, respectively. Then, when $t = 3 \times 10^{-10}$ s, the current density rises sharply, which indicates the occurrence of SEB. It is worth noting that the gate current density has not changed significantly during the whole simulation process. This result shows that the punch-through effect between source and drain, rather than between gate and drain, is the main reason for the SEB of p-GaN HEMT devices.

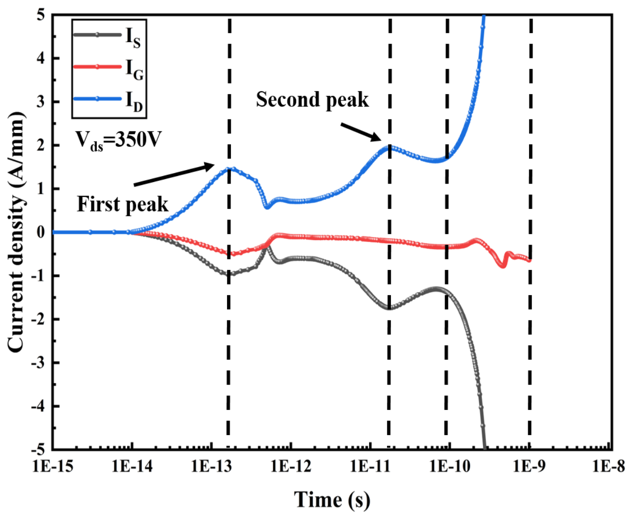

Fig. 9. Simulation plot of transient current density at source, drain and gate.

In order to study the dynamic behavior of carriers in the device after single event incident, we selected two current

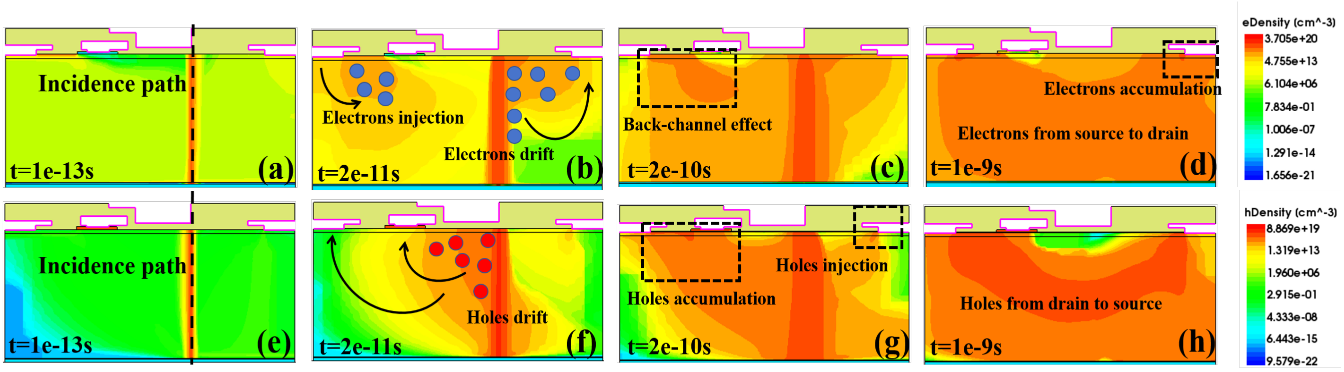

Fig. 10. Electron density distributions and hole density distributions at (a)(e) t = 1e-13 s, (b)(f) t = 2e-11 s, (c)(g) t = 2e-10 s , and (d)(h) t = 1e-9 s for Vds = 350V.

peaks and the key time points before and after SEB to analyze. When $t = 1 \times 10^{-13}$ s, a large number of electron-hole pairs are generated near the incident path of a single particle. These unbalanced carriers drift under the action of the internal electric field of the device, forming the first current peak. When $t = 2 \times 10^{-11}$ s, electrons move to the drain and holes move to the gate and source under the electric field. At the same time, we observed that a large number of hot electrons were injected into the device from the source, thus forming the second current peak. When $t = 2 \times 10^{-11}$ s, a large number of holes migrate to the vicinity of the source and gate and some holes are injected into the device from the drain. The accumulated holes near the source reduce the barrier of electron injection from the source to the buffer layer, leading to a more significant phenomenon of hot electron injection. This mechanism is called back-channel effect [32]. At the same time, the accumulation of holes near the gate reduces the potential barrier for electrons to cross the region under the gate from source, which is called bipolar effect [19]. These two charge enhancement effects significantly increase the possibility of punch-through between source and drain, as shown in Fig. 10(d) and Fig. 10(h).

Unbalanced carriers drift under the transverse electric field, and their drift behavior will further affect the distribution of transverse electric field. Fig. 11(a). demonstrates the variation of the transverse electric field distribution in the channel region with transient time. At $t = 1 \times 10^{-13}$ s, the high electric field region is mainly concentrated on the drain side of the field plate. With time, a large number of electrons move toward the drain, leading to the gradual migration of the center of the high electric field toward the drain. At the same time, significant collisional ionization of electrons occurs under the acceleration of the high electric field, leading to a sharp increase in electron density. At $t = 1 \times 10^{-9}$ s, the center of the high electric field and collision ionization center has migrated to the vicinity of the drain electrode, at which time the electric field strength in the channel region significantly exceeds the critical electric field strength of GaN (3.4 MV/cm). The combined effect of high electric field and high collisional ionization rate leads to material damage, which is the main reason for the drain leakage and penetration phenomena observed in Fig. 7(a).

Fig. 11(b). demonstrates the variation of the transverse electric field distribution in the barrier layer with transient time. During the transient time, the region near the gate is susceptible to a localized high electric field, which may exceed the critical electric field strength (5 MV/cm) of the AlGaN material, thus triggering material damage. This mechanism is the root cause of the increase in gate leakage current observed in Fig. 7(b).

IV. SYNERGISTIC EFFECT EXPERIMENT TEST AND ANALYSIS

1. Synergistic experiment setups

One of the main challenges faced by power devices when they are applied to the space environment is the radiation effect of multiple rays and energetic particles. In order to investigate the synergistic effect TID and SEE, a synergistic effect experiment was designed in this study. In the experiment, a group of devices were irradiated with γ-ray under Semi-ON bias conditions with a cumulative dose of $1\ \mathrm{Mrad(Si)}$. Subsequently, SEE experiment was performed immediately after the TID experiment was completed within two hours. The radiation conditions for the SEE experiment were consistent with SEB experiment, with the source and gate bias voltages set to $0\,\mathrm{V}$ and the drain voltage set to $100\,\mathrm{V}$during irradiation.The transfer characteristics and the gate leakage current of the devices were tested in detail before and after each experiment.

2. Results and analysis of synergistic experiment

The experimental results in Fig. 12. show that the threshold voltage of the device exhibits a significant positive drift with increasing γ-ray irradiation dose. However, in the subsequent SEE experiments, the threshold voltage undergoes a negative drift, which is similar to the results at a dose of $500\ \mathrm{Krad(Si)}$. It is noteworthy that the off-state leakage current significantly

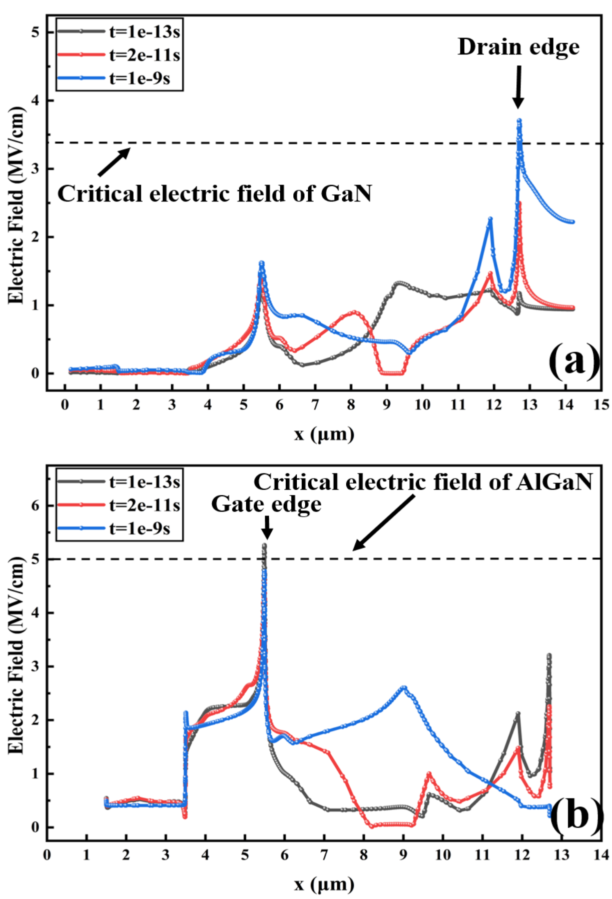

Fig. 11. Electric field distribution of channel layer (a) and barrier layer (b) at different time.

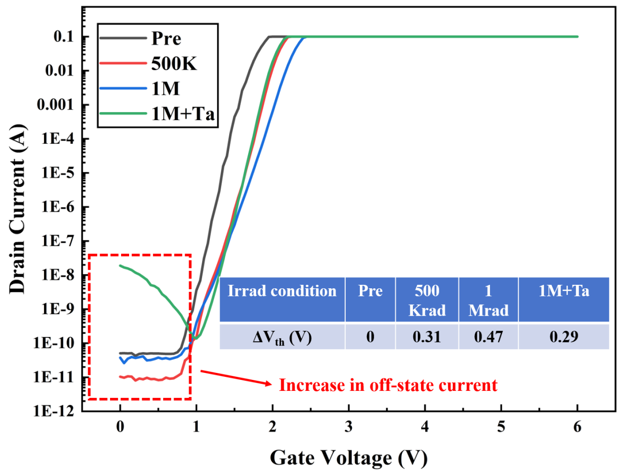

Fig. 12. Transfer characteristic curves and threshold voltage drifts at each stage of the synergistic experiment.

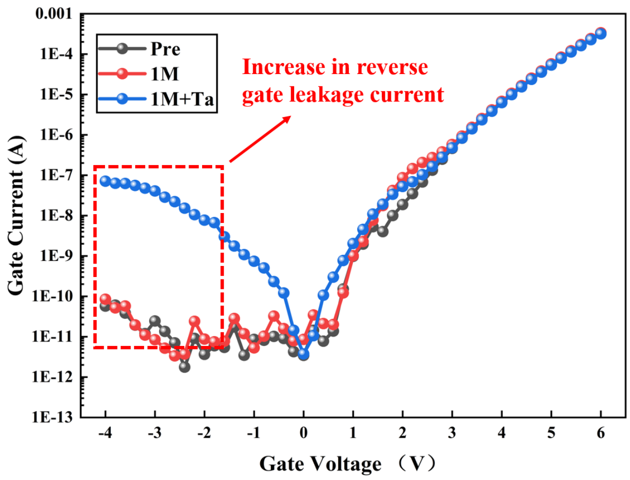

Fig. 13. Gate leakage current at each stage of the synergistic experiment.

increases by nearly three orders of magnitude after the synergistic effect experiment compared to the TID experiment alone. This phenomenon suggests that the synergistic effect of TID and SEE manifests itself as a superimposed effect of them. Specifically, SEE triggers material damage in the GaN layer of the device, including atomic displacement and even crack formation, which increases the leakage path of electrons in the off-state, leading to a significant increase in the off-state current and a negative drift of the threshold voltage. This is consistent with the results in Fig. 11(a).

The gate leakage current is shown in Fig. 13. The TID experiment resulted in a small increase in leakage current at positive low voltage, while the reverse gate leakage current did not change significantly. After further SEE experiments, there is no significant change in the forward gate current, and the reverse gate current increases dramatically by about three orders of magnitude. Based on the previous analysis, it is concluded that the irradiated p-i-n heterojunction degrades severely, while the Schottky junction maintains its function. This is related to the material damage in AlGaN barrier layer due to the high electric field shown in Fig. 11(b).

V. SUMMARY

In this paper, we performed SEB experiments and TID experiments on our self-developed P-GaN HEMT. The experimental results show that the SEB phenomenon manifests itself as an uncontrollable increase in the current between the source and drain but not between the gate and drain. The local electric field enhancement due to the charge enhancement effect and charge collection phenomenon as well as the intensification of collisional ionization are the main causes of material damage and devices failure. In TID experiments, electron trapping and hole trapping at the P-GaN/AlGaN interface and in the AlGaN barrier layer lead to threshold voltage drift, and the two competing mechanisms together determine the threshold voltage drift characteristics of the device. And the threshold voltage drift becomes more obvious as the gate bias voltage increases, while the gate leakage current is relatively

stable. In addition, we also carried out experiments on the synergistic effects of Ta ions and ^{60}Co γ-ray, and the results show that the two irradiation effects exhibit a superposition in devices, which further reveals the reliability degradation mechanism of P-GaN HEMTs under complex radiation environments.

---

[1] K. J. Chen, O. Häberlen, A. Lidow et al., GaN-on-Si Power Technology: Devices and Applications. IEEE Trans. Electron Devices. **64**, 779-795 (2017). doi: 10.1109/TED.2017.2657579

[2] I. Hwang, J. Kim, H. S. Choi et al., p-GaN Gate HEMTs With Tungsten Gate Metal for High Threshold Voltage and Low Gate Current. IEEE Electron Device Lett. **34**, 202-204 (2013). doi: 10.1109/LED.2012.2230312

[3] P. Wan, J. Yang, H. Lv et al., The Study of Displacement Damage in AlGaN/GaN High Electron Mobility Transistors Based on Experiment and Simulation Method. IEEE Trans. Nucl. Sci. **69**, 779-795 (2017). doi: 10.1109/TNS.2022.3144495

[4] T. Nelson, D. G. Georgiev, M. R. Hontz et al., Examination of Trapping Effects on Single-Event Transients in GaN HEMTs, IEEE Trans. Nucl. Sci. **70**, 328-335 (2017)doi: 10.1109/TNS.2022.3220235

[5] J. Millán, P. Godignon, X. Perpiñà et al., A Survey of Wide Bandgap Power Semiconductor Devices. IEEE Trans. Power Electron. **29**, 2155-2163 (2014). doi: 10.1109/TPEL.2013.2268900

[6] B-J. Kim, H-Y. Kim, J. Kim et al., Neutron irradiation on AlGaN/GaN high electron mobility transistors on SiC substrates. J. Cryst. Growth. **326**, 205–207 (2011). doi: 10.1109/LED.2009.2014473

[7] P-P. Hu, L-J. Xu, and S-X. Zhang et al., Failure mechanisms of AlGaN/GaN HEMTs irradiated by high-energy heavy ions with and without bias. NUCL SCI TECH. **36**, 1–10 (2025). doi: 10.1007/s41365-024-01567-2

[8] L-Q. Zhang, C-H.Zhang, C-L. Xu et al., Damage produced on GaN surface by highly charged Kr^{q+} irradiation. NUCL SCI TECH. **28**, 176 (2017). doi: 10.1007/s41365-017-0326-4

[9] G-P. Liu, X. Wang, M-N. Li et al.,Effects of high-energy proton irradiation on separate absorption and multiplication GaN avalanche photodiode. NUCL SCI TECH. **29**, 139 (2018). doi:10.1007/s41365-018-0480-3

[10] C. Y. Yang, C. H. Chung, W. Yu et al., A Comprehensive Study of Total Ionizing Dose Effect on the Electrical Performance of the GaN MIS-HEMT. IEEE Trans. Device Mater. Reliab. **22**, 276-281 (2022). doi: 10.1109/TDMR.2022.3173000.

[11] S. Abubakkar, and N. Zabah, and Y. Abdullah et al.,Effects of electron radiation on commercial power MOSFET with buck converter application. NUCL SCI TECH. **28**, 31 (2017). doi:10.1007/s41365-017-0189-8

[12] Y. Jiao, LH. Mo, JH. Yang et al., Heavy ion energy influence on multiple-cell upsets in small sensitive volumes: from standard to high energies. NUCL SCI TECH.**35**, 85 (2024). doi: 10.1007/s41365-024-01427-z

[13] ZG. Zhang, Y. Huang , YF. En et al., Investigation of maximum proton energy for qualified ground-based evaluation of single-event effects in SRAM devices. NUCL SCI TECH . **30**, 47 (2019). doi: 10.1007/s41365-019-0570-x .

[14] Y-P. Wang, Y-H. Luo, W. Wang et al., 60Co gamma radiation effect on AlGaN/AlN/GaN HEMT devices. Chin. Phys. C. 056201 (2013). doi: 10.1088/1674-1137/37/5/056201

[15] R. Jiang, E. X. Zhang, M. W. McCurdy et al., Dose-Rate Dependence of the Total-Ionizing-Dose Response of GaN-Based HEMTs. IEEE Trans. Nucl. **66**, 170–176 (2019). doi: 10.1109/TNS.2018.2873059 .

[16] H. Wu, X. Fu, J. Guo et al., Total Ionizing Dose and Annealing Effects on Shift for p-GaN Gate AlGaN/GaN HEMTs. IEEE Electron Device Lett. **43**, 1945–1948 (2022). doi: 10.1109/LED.2022.3205318.

[17] S. J. Cai, Y. S. Tang, R. Li et al., Annealing behavior of a proton irradiated $Al_xGa_{1-x}N$/GaN high electron mobility transistor grown by MBE. IEEE Trans. Electron Devices. **47**, 304–307 (2000). doi: 10.1109/16.822272.

[18] Y. Wang, X. -X. Fei, X. Wu et al., Simulation Study of Single-Event Burnout in GaN MISFET With Schottky Element. IEEE Trans. Electron Devices. **67**, 5466–5471 (2020). doi: 10.1109/TED.2020.3027533.

[19] Z. Zhen, C. Feng, Q. Wang et al., Single Event Burnout Hardening of Enhancement Mode HEMTs With Double Field Plates. IEEE Trans. Nucl. Sci. **68**, 2358-2366 (2021). doi: 10.1109/TNS.2021.3102980 .

[20] L. Sayadi, G. Iannaccone, S. Sicre et al., Threshold Voltage Instability in p-GaN Gate AlGaN/GaN HFETs. IEEE Trans. Electron Devices. **65**, 2454–2460 (2018). doi: 10.1109/TED.2018.2828702.

[21] QQ. Wang, HX. Liu, SP.Chen et al, Effects of total dose irradiation on the threshold voltage of H-gate SOI NMOS devices. NUCL SCI TECH. **27**, 117 (2016). doi: 10.1007/s41365-016-0110-x

[22] B. Li, H. Li, J. Wang et al., Asymmetric Bipolar Injection in a Schottky-Metal/p-GaN/AlGaN/GaN Device Under Forward Bias. IEEE Electron Device Lett. **40**, 1389-1392 (2019). doi: 10.1109/LED.2019.2926503.

[23] A. N. Tallarico, S. Stoffels, N. Posthuma et al., PBTI in GaN-HEMTs With p-Type Gate: Role of the Aluminum Content on ΔV_{TH} and Underlying Degradation Mechanisms. IEEE Trans. Electron Devices. **65**, 38–44 (2018). doi: 10.1109/TED.2017.2769167.

[24] X. Zhou, Z. Wang, Z. Wu et al., Total-Ionizing-Dose Radiation Effect on Dynamic Threshold Voltage in p-GaN Gate HEMTs. IEEE Trans. Electron Devices. **70**, 4081–4086 (2023). doi: 10.1109/TED.2023.3285515.

[25] A. Sarkar, Y. M. Haddara, Modeling of forward gate leakage current for normally off pGaN/AlGaN/GaN HEMTs. Solid-State Electron. **196**, 108420 (2022). doi: 10.1016/j.sse.2022.108420 .

[26] N. Xu, R. Hao, F. Chen et al., Gate leakage mechanisms in normally off p-GaN/AlGaN/GaN high electron mobility transistors. Appl. Phys. Lett. **113**, 152104 (2018). doi: 10.1063/1.5041343 .

[27] BC. Wang, CX. Tang and MT. Qiu, A machine learning approach to TCAD model calibration for MOSFET. NUCL SCI TECH. **34**, 1928 (2023). doi: 10.1007/s41365-023-01340-x.

[28] J. Li, Y. Wang, X-X. Fei et al., TCAD analysis of single-event burnout caused by heavy ions for a GaN HEMT.J. Comput. Electron. **24**, 38 (2025). doi: 10.1007/s10825-024-02275-1 .

[29] S. Liu, Y. Wang, X. Fei et al., Analysis and simulation of bulk polarization mechanism in p-GaN HEMT with Al component gradient buffer layer. Semicond. Sci. Technol. **39**, 075021 (2024). doi: 10.1088/1361-6641/ad5580.

[30] X-X. Fei, Y. Wang, B. Sun et al., Simulation study of single-event burnout in hardened GaN MISFET. Radiat. Phys. Chem. **213**, 111244 (2023). doi: 10.1016/j.radphyschem.2023.111244.

[31] X-X. Fei, Y. Wang, X. Luo et al., Research of single-event burnout and hardened GaN MISFET with embedded PN junction. Microelectron. Reliab. **110**, 113699 (2020). doi: 10.1016/j.microrel.2020.113699.

[32] X. Luo, Y. Wang, Y. Hao et al., Research of Single-Event Burnout and Hardening of AlGaN/GaN-Based MISFET. IEEE Trans. Electron Devices. **66**, 1118–1122 (2019). doi: 10.1109/TED.2018.2887245.

[33] F. Zhang, Y. Wang, X. Wu et al., An SEB Hardened AlGaN/GaN HEMT With Barrier Interlayer. IEEE Access, **8**,12445–12451 (2020). doi: 10.1109/ACCESS.2020.2964948.